

Benefit of Joint DOA and Delay Estimation with Application to Indoor Localization in WiFi and 5G

Fei Wen Peilin Liu

Department of Electronic Engineering
Shanghai Jiao Tong University, Shanghai, China
wenfei@sjtu.edu.cn; liupeilin@sjtu.edu.cn

Haichao Wei Yi Zhang

Huawei Technologies Co., Ltd
Shanghai, China
weihaichao@huawei.com; aabear@huawei.com

Abstract—Accurate indoor localization has long been a challenging problem due to the presence of multipath. Joint direction-of-arrival (DOA) and time delay (TD) estimation is a promising technique for accurate indoor Localization in next generation WiFi and 5G, as it has the capability of separating the line-of-sight (LOS) signal from multipath signals in the TD space. Although the benefit of joint DOA and TD estimation over DOA-only estimation has been empirically shown long ago, it has not been theoretically justified yet. In this paper, we provide a theoretical proof of the benefit of joint DOA and TD estimation over DOA-only estimation. Further, experimental results with simulated WiFi setting have been provided to demonstrate the theoretical finding. Matlab code is available at <https://github.com/FWen/JADE.git>.

Index Terms—Direction-of-arrival estimation, time delay estimation, 5G, WiFi, multipath, indoor localization, channel state information.

I. INTRODUCTION

WiFi and mobile communication networks based localization has a promising prospect due to their wide coverage both indoors and outdoors and good universality for various user terminals. Accurate localization in harsh indoor environments is expected to be achieved in next generation WiFi and 5G networks [1]–[4]. In next generation WiFi and 5G, two favorable opportunities arise for achieving high-accuracy indoor localization. First, WiFi access points and 5G base stations are incorporating ever-increasing numbers of antennas to bolster capacity and coverage with MIMO techniques. Second, the used signals have wider bandwidth (e.g., towards one hundred MHz or even more). More antennas facilitate accurate direction-of-arrival (DOA) estimation. Meanwhile, wider bandwidth facilitates accurate time delay (TD) estimation and, more importantly, facilitates reliable separation of the line-of-sight (LOS) signal from multipath signals. Besides, dense deployment of access points or base stations is a tendency in next generation WiFi and 5G networks, which facilitates the application of multiple station fusion based localization techniques [5], [21]. In this context, joint azimuth, elevation angles and TD estimation becomes a key technique for high-accuracy 3-dimensional (3D) indoor localization in next generation WiFi and 5G networks [2]–[4].

In the past two decades, a number of methods for joint DOA and TD estimation have been proposed [6]–[20]. Compared with traditional DOA-only estimation methods (e.g., [21]–

[23]), joint DOA and TD estimation methods have shown significant superiority, since such methods fully exploit the spatial diversity as well as temporal diversity in estimating the multipath channel. This advantage of joint DOA and TD estimation has been demonstrated in numerous simulation results. However, it has not been theoretically justified yet.

The goal of this paper is to give a theoretical justification on the benefit of joint DOA and TD estimation over DOA-only estimation. First, the CRB for joint DOA and TD estimation has been provided in closed-form, based on which we further provide analysis to show the advantage of joint DOA and TD estimation over DOA-only estimation. Although such advantage has been empirically shown long ago, our analysis is the first theoretical proof of it.

II. SIGNAL MODEL

Consider an M sensor array receiving L reflections of a far-field signal $s(t)$ with TDs τ_1, \dots, τ_L , incident DOA angles $\theta_1, \dots, \theta_L$. The complex snapshot of the m -th sensor at time t_n can be modeled as

$$x_m(t_n) = \sum_{l=1}^L \beta_l a_m(\theta_l) s(t_n - \tau_l) + w_m(t_n) \quad (1)$$

for $n = 1, \dots, N$, where β_l is a complex coefficient representing the attenuation factor (phase shift and amplitude attenuation) of the l -th reflection. The complex channel fading are assumed to be constant within a data burst such that β_l , $l \in \{1, \dots, L\}$, is not dependent on t . The complex signal $s(t)$ is known. $w_m(t_n)$ is zero-mean white Gaussian noise which is independent to the source signal. Let $\mathbf{x}(t_n) = [x_1(t_n), \dots, x_M(t_n)]^T$, $\mathbf{w}(n) = [w_1(t_n), \dots, w_M(t_n)]^T$, $\mathbf{a}(\theta) = [a_1(\theta), \dots, a_M(\theta)]^T$, the array outputs can be expressed as

$$\mathbf{x}(t_n) = \sum_{l=1}^L \beta_l \mathbf{a}(\theta_l) s(t_n - \tau_l) + \mathbf{w}(t_n). \quad (2)$$

In the frequency-domain, the signal of the m -th sensor at the k -th frequency bin (or subcarrier), $0 \leq k \leq K$, can be modeled as

$$X_m(\omega_k) = \sum_{l=1}^L \beta_l a_m(\theta_l) S(\omega_k) e^{-j\omega_k \tau_l} + W_m(\omega_k) \quad (3)$$

where K is the number of the effective frequency bins (or subcarriers) of the signal, $X_m(\omega_k)$, $S(\omega_k)$ and $W_m(\omega_k)$ are respectively the discrete Fourier transform (DFT) of $x_m(t_n)$, $s(t_n)$ and $w_m(t_n)$. In a vector form, the array outputs in the frequency-domain can be expressed as

$$\mathbf{x}(k) = \mathbf{D}(k)\boldsymbol{\beta} + \mathbf{w}(k) \quad (4)$$

where $\boldsymbol{\beta} = [\beta_1, \dots, \beta_L]^T$ and $\mathbf{x}(k) = [X_1(\omega_k), \dots, X_M(\omega_k)]^T$, $\mathbf{w}(k) = [W_1(\omega_k), \dots, W_M(\omega_k)]^T$, $\mathbf{D}(k) = [\mathbf{a}(\theta_1)e^{-j\omega_k\tau_1}, \dots, \mathbf{a}(\theta_L)e^{-j\omega_k\tau_L}]S(\omega_k)$.

III. APPROXIMATE MAXIMUM LIKELIHOOD ALGORITHM

Assume the noise spectrum vector $\mathbf{w}(k)$ is zero-mean circularly complex Gaussian distributed with variance σ^2 in each element, i.e., $E\{\mathbf{w}(k)\mathbf{w}^H(k)\} = \sigma^2\mathbf{I}_M$ and $E\{\mathbf{w}(k)\mathbf{w}^T(k)\} = \mathbf{0}_M$ for $k = 0, \dots, K$. Let $\boldsymbol{\theta} = [\theta_1, \dots, \theta_L]^T$, $\boldsymbol{\tau} = [\tau_1, \dots, \tau_L]^T$ and $\boldsymbol{\Omega} = [\boldsymbol{\theta}^T, \boldsymbol{\tau}^T, \beta^T, \sigma^2]^T$ which contains all the unknown parameters in the model. Then, the likelihood function of $\boldsymbol{\Omega}$ can be expressed as

$$f(\boldsymbol{\Omega}) = \frac{1}{(\pi\sigma^2)^{MN}} \exp\left\{-\frac{1}{\sigma^2} \sum_{k=1}^K \|\mathbf{g}(k)\|^2\right\}$$

with $\mathbf{g}(k) = \mathbf{x}(k) - \mathbf{D}(k)\boldsymbol{\beta}$. The according log-likelihood is

$$\mathcal{L}(\boldsymbol{\Omega}) = -MN \log \sigma^2 - \frac{1}{\sigma^2} \sum_{k=1}^K \|\mathbf{g}(k)\|^2$$

and the ML estimator for $\boldsymbol{\Omega}$ is given by

$$\hat{\boldsymbol{\Omega}} = \arg \max_{\boldsymbol{\Omega}} \mathcal{L}(\boldsymbol{\Omega}).$$

As the dependency of the log-likelihood function with respect to $\boldsymbol{\theta}$, $\boldsymbol{\tau}$ and $\boldsymbol{\beta}$ is through $\|\mathbf{g}(k)\|^2$, and $\|\mathbf{g}(k)\|^2$ is independent of σ^2 , the concentrated ML estimator for $\boldsymbol{\theta}$, $\boldsymbol{\tau}$ and $\boldsymbol{\beta}$ is given by

$$(\hat{\boldsymbol{\theta}}, \hat{\boldsymbol{\tau}}, \hat{\boldsymbol{\beta}}) = \arg \min_{\boldsymbol{\theta}, \boldsymbol{\tau}, \boldsymbol{\beta}} \sum_{k=1}^K \|\mathbf{g}(k)\|^2. \quad (5)$$

Next, we introduce the AML algorithm [6], which approximately solves the ML formulation. Define $\mathbf{A}(\boldsymbol{\theta}) = [\mathbf{a}(\theta_1), \dots, \mathbf{a}(\theta_L)]$, $\mathbf{r}(k, \boldsymbol{\tau}) = [e^{-j\omega_k\tau_1}, \dots, e^{-j\omega_k\tau_L}]^T S(\omega_k)$ and

$$\mathbf{u}(k, \boldsymbol{\tau}) = \text{diag}\{\boldsymbol{\beta}\}\mathbf{r}(k, \boldsymbol{\tau}) \quad (6)$$

$$\mathbf{B} = \mathbf{A}(\boldsymbol{\theta})\text{diag}\{\boldsymbol{\beta}\}. \quad (7)$$

First, the AML algorithm derives an estimator for $\boldsymbol{\theta}$, and $\boldsymbol{\beta}$ conditioned on $\boldsymbol{\tau}$. Specifically, given an estimation of $\boldsymbol{\tau}$, denoted by $\hat{\boldsymbol{\tau}}$, the minimization problem (5) can be rewritten as

$$(\hat{\boldsymbol{\theta}}, \hat{\boldsymbol{\beta}}) = \arg \min_{\boldsymbol{\theta}, \boldsymbol{\beta}} \sum_{k=1}^K \|\mathbf{x}(k) - \mathbf{B}\mathbf{r}(k, \hat{\boldsymbol{\tau}})\|^2. \quad (8)$$

Instead of minimizing (8) directly with respect to $\boldsymbol{\theta}$ and $\boldsymbol{\beta}$, we minimize it first with respect to the unstructured matrix \mathbf{B} , for

which the explicit solution is given by

$$\hat{\mathbf{B}} = \left[\sum_{k=1}^K \mathbf{x}(k)\mathbf{r}^H(k, \hat{\boldsymbol{\tau}}) \right] \left[\sum_{k=1}^K \mathbf{r}(k, \hat{\boldsymbol{\tau}})\mathbf{r}^H(k, \hat{\boldsymbol{\tau}}) \right]^{-1}. \quad (9)$$

Let $\hat{\mathbf{b}}_l$ denote the l -th column of $\hat{\mathbf{B}}$, i.e., $\hat{\mathbf{B}} = [\hat{\mathbf{b}}_1, \dots, \hat{\mathbf{b}}_L]$. From (7), only the l -th column of \mathbf{B} is dependent on θ_l , and β_l . Thus, given an estimation $\hat{\mathbf{B}}$, we can estimate θ_l and β_l via the following formulation

$$(\hat{\theta}_l, \hat{\beta}_l) = \arg \min_{\theta, \beta} \|\hat{\mathbf{b}}_l - \beta\mathbf{a}(\theta)\|^2. \quad (10)$$

for $l = 1, \dots, L$. The solution to (10) is given by

$$\hat{\theta}_l = \arg \max_{\theta} \frac{\|\hat{\mathbf{b}}_l^H \mathbf{a}(\theta)\|^2}{\|\mathbf{a}(\theta)\|^2} \quad (11)$$

and

$$\hat{\beta}_l = \frac{\mathbf{a}^H(\hat{\theta}_l)\hat{\mathbf{b}}_l}{\|\mathbf{a}(\hat{\theta}_l)\|^2}. \quad (12)$$

Next, we estimate $\boldsymbol{\tau}$ and $\boldsymbol{\beta}$ conditioned on $\boldsymbol{\theta}$. Specifically, given an estimation of $\boldsymbol{\theta}$, denoted by $\hat{\boldsymbol{\theta}}$, the minimization problem (5) can be rewritten as

$$(\hat{\boldsymbol{\tau}}, \hat{\boldsymbol{\beta}}) = \arg \min_{\boldsymbol{\tau}, \boldsymbol{\beta}} \sum_{k=1}^K \|\mathbf{x}(k) - \mathbf{A}(\hat{\boldsymbol{\theta}})\mathbf{u}(k, \boldsymbol{\tau})\|^2. \quad (13)$$

In a similar manner to (10), we do not minimize (13) directly with respect to $\boldsymbol{\tau}$ and $\boldsymbol{\beta}$ rather than minimize it first with respect to the unstructured vectors $\mathbf{u}(k, \boldsymbol{\tau})$ for $k = 1, \dots, K$, which yields the following explicit solution

$$\hat{\mathbf{u}}(k, \boldsymbol{\tau}) = [\mathbf{A}^H(\hat{\boldsymbol{\theta}})\mathbf{A}(\hat{\boldsymbol{\theta}})]^{-1} \mathbf{A}^H(\hat{\boldsymbol{\theta}})\mathbf{x}(k). \quad (14)$$

Define

$$\hat{\mathbf{V}} = [\hat{\mathbf{v}}_1, \dots, \hat{\mathbf{v}}_L] = \begin{bmatrix} \hat{\mathbf{u}}^T(1, \boldsymbol{\tau})/S(\omega_1) \\ \vdots \\ \hat{\mathbf{u}}^T(K, \boldsymbol{\tau})/S(\omega_K) \end{bmatrix}.$$

From (6), the dependency of $\mathbf{u}(k, \boldsymbol{\tau})$ with respect to τ_l and β_l is only through the l -th element of $\mathbf{u}(k, \boldsymbol{\tau})$. Thus, given an estimation $[\hat{\mathbf{v}}_1, \dots, \hat{\mathbf{v}}_L]$, we can estimate τ_l and β_l via the following formulation

$$(\hat{\tau}_l, \hat{\beta}_l) = \arg \min_{\tau, \beta} \|\hat{\mathbf{v}}_l - \beta\mathbf{t}(\tau)\|^2 \quad (15)$$

for $l = 1, \dots, L$, where $\mathbf{t}(\tau) = [e^{-j\omega_1\tau}, \dots, e^{-j\omega_K\tau}]^T$. The solution to (15) is given by

$$\hat{\tau}_l = \arg \max_{\tau} \|\mathbf{t}^H(\tau)\hat{\mathbf{v}}_l\|^2 \quad (16)$$

and

$$\hat{\beta}_l = \frac{1}{N} \mathbf{t}^H(\hat{\tau}_l)\hat{\mathbf{v}}_l. \quad (17)$$

The AML algorithm alternatively update the steps, first the TDs via (14) and (16), then the DOAs via (9) and (11). This algorithm can achieve satisfactory performance within only a few iterations.

IV. CRB AND ANALYSIS

This section provides CRB and analysis on the advantage of joint DOA and TD estimation over DOA-only estimation. The proof will be presented in a later work [24].

A. Cramer-Rao Bound

1) *CRB for joint DOA and TD estimation*: Denote

$$\begin{aligned} \mathbf{D}(k) &= S(\omega_k) [\mathbf{d}_k(\theta_1, \tau_1), \dots, \mathbf{d}_k(\theta_L, \tau_L)] \\ \mathbf{\Gamma}_1 &= \Re \left\{ \left(\tilde{\mathbf{E}}^H \mathbf{P}_{\tilde{\mathbf{D}}}^\perp \tilde{\mathbf{E}} \right) \odot (\boldsymbol{\beta}^* \boldsymbol{\beta}^T) \right\} \\ \mathbf{\Gamma}_2 &= \Re \left\{ \left(\tilde{\mathbf{E}}^H \mathbf{P}_{\tilde{\mathbf{D}}}^\perp \tilde{\mathbf{\Lambda}} \right) \odot (\boldsymbol{\beta}^* \boldsymbol{\beta}^T) \right\} \\ \mathbf{\Gamma}_3 &= \Re \left\{ \left(\tilde{\mathbf{\Lambda}}^H \mathbf{P}_{\tilde{\mathbf{D}}}^\perp \tilde{\mathbf{\Lambda}} \right) \odot (\boldsymbol{\beta}^* \boldsymbol{\beta}^T) \right\} \end{aligned}$$

where $\mathbf{d}_k(\theta, \tau) = \mathbf{a}(\theta) e^{-j\omega_k \tau}$ and

$$\begin{aligned} \mathbf{P}_{\tilde{\mathbf{D}}}^\perp &= \mathbf{I}_{MK} - \tilde{\mathbf{D}}(\tilde{\mathbf{D}}^H \tilde{\mathbf{D}})^{-1} \tilde{\mathbf{D}}^H \\ \tilde{\mathbf{E}} &= [\mathbf{E}^T(1), \dots, \mathbf{E}^T(K)]^T \\ \tilde{\mathbf{\Lambda}} &= [\mathbf{\Lambda}^T(1), \dots, \mathbf{\Lambda}^T(K)]^T \\ \tilde{\mathbf{D}} &= [\mathbf{D}^T(1), \dots, \mathbf{D}^T(K)]^T \end{aligned}$$

with

$$\begin{aligned} \mathbf{E}(k) &= S(\omega_k) \left[\frac{\partial \mathbf{d}_k(\theta_1, \tau_1)}{\partial \theta_1}, \dots, \frac{\partial \mathbf{d}_k(\theta_L, \tau_L)}{\partial \theta_L} \right] \\ \mathbf{\Lambda}(k) &= S(\omega_k) \left[\frac{\partial \mathbf{d}_k(\theta_1, \tau_1)}{\partial \tau_1}, \dots, \frac{\partial \mathbf{d}_k(\theta_L, \tau_L)}{\partial \tau_L} \right]. \end{aligned}$$

The CRB formulae for the DOA and TD are given as follows.

Theorem 1: The $L \times L$ deterministic CRB matrix for the DOAs is given by

$$\mathbf{CRB}_{\boldsymbol{\theta}\boldsymbol{\theta}}^J = \frac{\sigma^2}{2} (\mathbf{\Gamma}_1 - \mathbf{\Gamma}_2 \mathbf{\Gamma}_3^{-1} \mathbf{\Gamma}_2^T)^{-1} \quad (18)$$

and the $L \times L$ deterministic CRB matrix for the TDs is given by

$$\mathbf{CRB}_{\boldsymbol{\tau}\boldsymbol{\tau}}^J = \frac{\sigma^2}{2} (\mathbf{\Gamma}_3 - \mathbf{\Gamma}_2^T \mathbf{\Gamma}_1^{-1} \mathbf{\Gamma}_2)^{-1}. \quad (19)$$

2) *CRB for DOA-only estimation*: Rewrite the model (4) as

$$\mathbf{x}(k) = \mathbf{A}(\boldsymbol{\theta}) \mathbf{c}(k) + \mathbf{w}(k) \quad (20)$$

where $\mathbf{c}(k) = [\beta_1 e^{-j\omega_k \tau_1} S(\omega_k), \dots, \beta_L e^{-j\omega_k \tau_L} S(\omega_k)]^T$. Then, treating $\mathbf{c}(k)$ as the unknown source signals, we can estimate the DOA using a traditional DOA-only estimator without the consideration of the TD. In this case, the deterministic CRB for DOA-only estimation is given by [25]

$$\mathbf{CRB}_{\boldsymbol{\theta}\boldsymbol{\theta}}^O = \frac{\sigma^2}{2K} \left[\Re \left\{ \left(\Psi^H \mathbf{P}_{\mathbf{A}}^\perp \Psi \right) \odot \mathbf{R}_{\tilde{\mathbf{c}}} \right\} \right]^{-1} \quad (21)$$

where $\tilde{\mathbf{c}}(k) = [\mathbf{c}^T(k), \mathbf{c}^T(k)]^T$, $\mathbf{P}_{\mathbf{A}}^\perp = \mathbf{I}_M - \mathbf{P}_{\mathbf{A}} = \mathbf{I}_M - \mathbf{A}(\mathbf{A}^H \mathbf{A})^{-1} \mathbf{A}$ and

$$\begin{aligned} \mathbf{R}_{\tilde{\mathbf{c}}} &= \frac{1}{K} \sum_{k=1}^K \tilde{\mathbf{c}}^*(k) \tilde{\mathbf{c}}^T(k) \\ \Psi &= \left[\frac{\partial \mathbf{a}(\theta_1)}{\partial \theta_1}, \dots, \frac{\partial \mathbf{a}(\theta_L)}{\partial \theta_L} \right]. \end{aligned}$$

B. Analysis

Intuitively, since joint DOA and TD estimation simultaneously exploits the DOA and TD structure of the multipath channels, the corresponding CRB (18) should be lower than or at least equal to the CRB (21) for DOA-only estimation. This is theoretically verified by the following results.

Theorem 2: The DOA-related block of CRB for joint DOA and TD estimation is bounded by the associated CRB for DOA-only estimation

$$\mathbf{CRB}_{\boldsymbol{\theta}\boldsymbol{\theta}}^J \leq \mathbf{CRB}_{\boldsymbol{\theta}\boldsymbol{\theta}}^O. \quad (22)$$

Further, if all the multipath signals have the same TD, i.e., $\tau_1 = \dots = \tau_L$, or in the particular case of a single path, i.e., $L = 1$, the equality in (22) is true.

Theorem 3: If all the multipath signals have the same TD, i.e., $\tau_1 = \dots = \tau_L$, then, the DOA-related block of CRB for joint DOA and TD estimation is equivalent to that for DOA-only estimation as

$$\begin{aligned} \mathbf{CRB}_{\boldsymbol{\theta}\boldsymbol{\theta}}^J &= \mathbf{CRB}_{\boldsymbol{\theta}\boldsymbol{\theta}}^O \\ &= \frac{\sigma^2}{2 \sum_{k=1}^K |S(\omega_k)|^2} \left[\Re \left\{ \left(\Psi^H \mathbf{P}_{\mathbf{A}}^\perp \Psi \right) \odot (\boldsymbol{\beta}^* \boldsymbol{\beta}^T) \right\} \right]^{-1}. \end{aligned} \quad (23)$$

Theorem 4: In the case of a single path, we have

$$\begin{aligned} \mathbf{CRB}_{\tau_1 \tau_1}^J &= \frac{\sigma^2 \sum_{k=1}^K |S(\omega_k)|^2}{2 |\beta_1|^2 \|\mathbf{a}(\theta_1)\|^2 \sum_{k=1}^K \sum_{n=1}^K \omega_k (\omega_k - \omega_n) |S(\omega_k)|^2 |S(\omega_n)|^2}. \end{aligned} \quad (24)$$

The results indicates that, when all the incident signals have the same TD or there exists only a single path $L = 1$, $\mathbf{CRB}_{\boldsymbol{\theta}\boldsymbol{\theta}}^J$ is independent on the TD and $\mathbf{CRB}_{\boldsymbol{\theta}\boldsymbol{\theta}}^J = \mathbf{CRB}_{\boldsymbol{\theta}\boldsymbol{\theta}}^O$ holds. Moreover, when $L = 1$, the CRB (23) for TD is independent on the DOA, and it is dependent on the signal bandwidth, sensor number, and signal power, which accords well with the well-established results for TD estimation [26]–[28]. The benefit of joint estimation mainly happens when there exist multiple reflections, i.e., $L > 1$, and the TDs of the multiple reflections are well separated. In practical indoor localization scenarios, since it is often the case that $L > 1$ and the line-of-sight (LOS) signal has a smaller value than that of the multipath signals, the LOS signal can be separated from the multipath signals in the TD space by joint DOA and TD estimation if the signal bandwidth is wide enough. In this sense, joint DOA and TD estimation can effectively suppress the effect of multipath on localization accuracy.

V. SIMULATION RESULTS

In this section, we evaluate the performance of the proposed AML algorithm and demonstrate the theoretical results via simulations. We consider a typical WiFi setting according to 802.11n, which operates in 5.32 GHz and uses 40 MHz

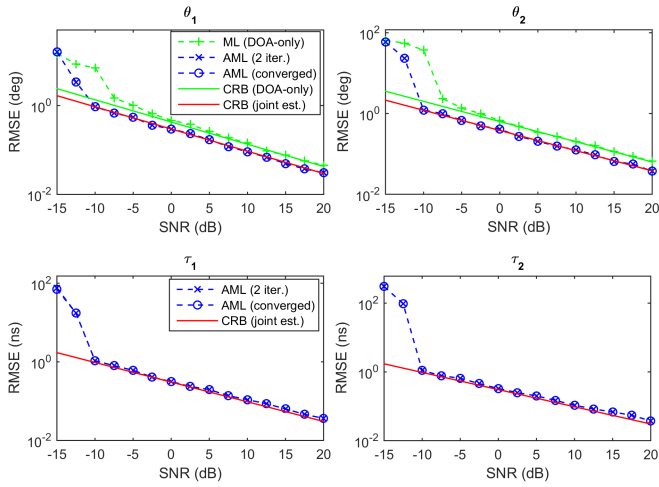


Fig. 1. RMSE of DOA and TD estimation versus SNR. Two paths with $\theta_1 = 30^\circ$, $\theta_2 = 40^\circ$, $\tau_1 = 50$ ns and $\tau_2 = 100$ ns.

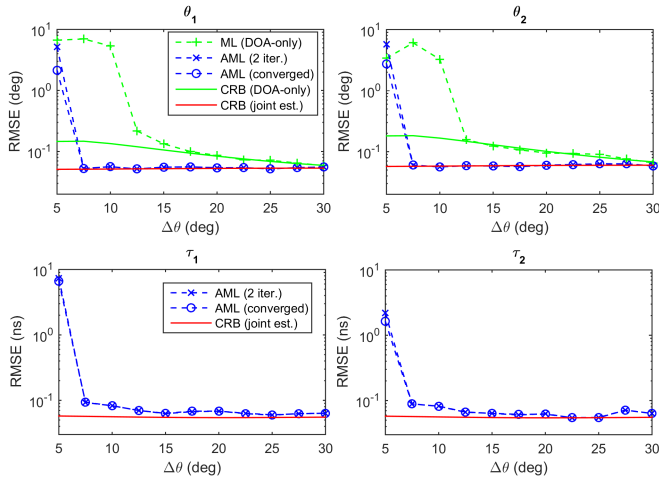


Fig. 2. RMSE of DOA and TD estimation versus DOA separation $\Delta\theta$. Two paths with $\theta_1 = 30^\circ$, $\theta_2 = \theta_1 + \Delta\theta$, $\tau_1 = 50$ ns and $\tau_2 = 80$ ns.

bandwidth with 128 subcarriers and the subcarrier frequency spacing is 312.5 KHz. In practical 802.11n WiFi system, only 114 subcarriers are used for 40 MHz bandwidth. A uniform circular array (UCA) of 16 omni-directional sensors with radius $r = 1.5\lambda$ is considered. The CSI at the subcarriers are generated as (4). Mutually independent zero-mean white Gaussian noise is added to control the signal-to-noise ratio (SNR). Each provided result is an average over 500 independent runs.

Two paths with attenuation factors $\beta_1 = e^{j\varphi_1}$ and $\beta_2 = 0.9e^{j\varphi_2}$, where the phase φ_1 and φ_2 are randomly selected from $[0, 2\pi]$. The DOAs of the two paths are $\theta_1 = 30^\circ$, $\theta_2 = 40^\circ$, and the time delays of the two paths are $\tau_1 = 50$ ns and $\tau_2 = 100$ ns, respectively. Fig. 1 shows the root mean square error (RMSE) of DOA and TD estimation for varying SNR. The AML algorithm gives significantly better performance than the DOA-only ML algorithm [29]. It indicates that joint estimation has the potential to significantly

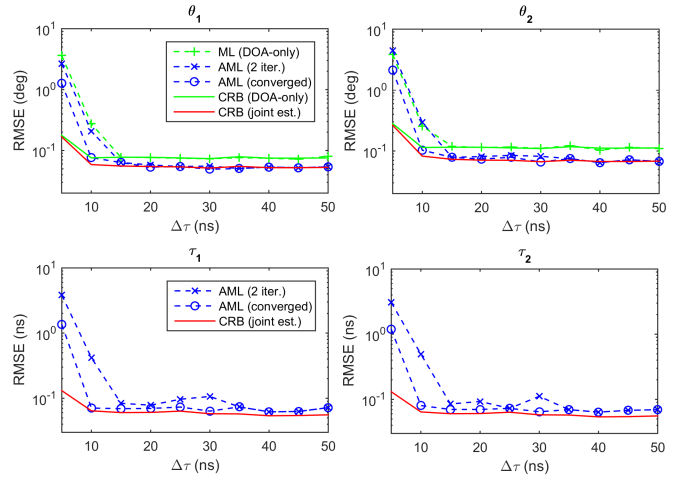


Fig. 3. RMSE of DOA and TD estimation versus TD separation $\Delta\tau$. SNR = 15 dB, two paths with $\theta_1 = 30^\circ$, $\theta_2 = 40^\circ$, $\tau_1 = 50$ ns and $\tau_2 = \tau_1 + \Delta\tau$ ns.

improve the DOA estimation accuracy compared with DOA-only estimation. Moreover, for the AML algorithm, only two iterations are enough for it to achieve satisfactory performance.

Fig. 2 presents the RMSE of DOA and TD estimation for varying DOA separation $\Delta\theta$ between the two paths. The DOAs of the two paths are $\theta_1 = 30^\circ$, $\theta_2 = \theta_1 + \Delta\theta$, and the time delays of the two paths are $\tau_1 = 50$ ns and $\tau_2 = 80$ ns, respectively. $\Delta\theta$ is varied from 5° to 30° . The SNR is 15 dB. The advantage of joint estimation over DOA-only estimation is especially conspicuous for small angular separation. When the multipaths are well separated in DOA, joint estimation and DOA-only estimation tend to give comparable performance.

Fig. 3 shows the RMSE of DOA and TD estimation for varying TD separation $\Delta\tau$ between the two paths. The DOAs of the two paths are $\theta_1 = 30^\circ$, $\theta_2 = 40^\circ$, and the time delays of the two paths are $\tau_1 = 50$ ns, $\tau_2 = \tau_1 + \Delta\tau$ ns, respectively. $\Delta\tau$ is varied from 5 ns to 50 ns. The SNR is 15 dB. It can be seen that, the difference between the CRBs of joint estimation and DOA-only estimation decreases as the TD separation decreases. The advantage of joint estimation over DOA-only estimation is prominent for relatively large TD separation.

VI. CONCLUSION

This addressed the joint DOA and TD estimation problem, which can be used for indoor localization in next generalization WiFi and 5G networks. We analytically proved the advantage of joint DOA and TD estimation over DOA-only estimation, which is the first theoretical proof of such advantage in the literature studying joint DOA and TD estimation. The results indicate that, the benefit due to joint estimation over DOA-only estimation arises when there exist multiple reflections and the time delays of the multiple reflections are well separated.

REFERENCES

- [1] Y. Rezgui, L. Pei, Xin Chen, et al., "An efficient normalized rank-based SVM for room level indoor WiFi localization with diverse devices," *Mobile Information Systems*, vol. 2017, pp. 1–19, 2017.
- [2] M. Koivisto, A. Hakkarainen, M. Costa, P. Kela, K. Leppanen, and M. Valkama, "High-efficiency device positioning and location-aware communications in dense 5G networks," *arXiv preprint*, arXiv:1608.03775, 2016.
- [3] M. Koivisto, M. Costa, J. Werner, K. Heiska, et al., "Joint device positioning and clock synchronization in 5G ultra-dense networks," *arXiv preprint*, arXiv:1604.03322, 2016.
- [4] M. Koivisto, M. Costa, A. Hakkarainen, et al., "Joint 3D positioning and network synchronization in 5G ultra-dense networks using UKF and EKF," *arXiv preprint*, arXiv:1608.03710, 2016.
- [5] F. Wen, W. Xie, X. Chen, and P. Liu, "DOA estimation for noncircular sources with multiple noncoherent subarrays," *IEEE Communications Letters*, vol. 21, pp. 1783–1786, May 2017.
- [6] M. Wax and A. Leshem, "Joint estimation of time delays and directions of arrival of multiple reflections of a known signal," *IEEE Trans. Signal Process.*, vol. 45, pp. 2477–2484, Oct. 1997.
- [7] M. C. Vanderveen, C. B. Papadias, and A. J. Paulraj, "Joint angle and delay estimation (JADE) for multipath signals arriving at an antenna array," *IEEE Commun. Lett.*, vol. 1, no. 1, pp. 12–14, Jan. 1997.
- [8] A. J. Van Der Veen, M. C. Vanderveen, and A. J. Paulraj, "Joint angle and delay estimation using shift-invariance properties," *IEEE Signal Processing Letters*, vol. 4, no. 5, pp. 142–145, 1997.
- [9] A. Swindlehurst, "Time delay and spatial signature estimation using known asynchronous signals," *IEEE Trans. Signal Process.*, vol. 46, no. 2, pp. 449–462, Feb. 1998.
- [10] G. G. Raleigh and T. Boros, "Joint space-time parameter estimation for wireless communication channels," *IEEE Trans. Signal Process.*, vol. 46, no. 5, pp. 1333–1343, May 1998.
- [11] A. Van der Veen, M. C. Vanderveen, and A. Paulraj, "Joint angle and delay estimation using shift-invariance techniques," *IEEE Trans. Signal Process.*, vol. 46, no. 2, pp. 405–418, Feb. 1998.
- [12] M. C. Vanderveen, A. Van der Veen, and A. Paulraj, "Estimation of multipath parameters in wireless communications," *IEEE Trans. Signal Process.*, vol. 46, no. 3, pp. 682–690, Mar. 1998.
- [13] Y.-F. Chen and M. D. Zoltowski, "Joint angle and delay estimation for DS-CDMA with application to reduced dimension space-time RAKE receivers," *IEEE Trans. Acoust. Speech Signal Process.*, vol. 5, pp. 2933–2936, March 1999.
- [14] Y. Y. Wang, J. T. Chen, and W. H. Fang, "TST-MUSIC for joint DOA-delay estimation," *IEEE Trans. Signal Process.*, vol. 49, pp. 721–729, Apr. 2001.
- [15] J. Picheral and U. Spagnolini, "Angle and delay estimation of space-time channels for TD-CDMA systems," *IEEE Trans. Wireless Commun.*, vol. 3, no. 3, pp. 758–769, May 2004.
- [16] A. N. Lemma, A.-J. van der Veen, and E. F. Deprettere, "Analysis of joint angle-frequency estimation using ESPRIT," *IEEE Trans. Signal Process.*, vol. 51, pp. 1264–1283, May 2003.
- [17] J. He, M. N. S. Swamy, and M. O. Ahmad, "Joint space-time parameter estimation for underwater communication channels with velocity vector sensor arrays," *IEEE Trans. Wireless Communications*, vol. 11, no. 11, pp. 3869–3877, Nov. 2012.
- [18] A. Bazzi, D. T. M. Slock, and L. Meilhac, "Efficient maximum likelihood joint estimation of angles and times of arrival of multiple paths," in *Proc. of IEEE GLOBECOM Workshop on Localization for Indoors, Outdoors, and Emerging Networks*, 2015.
- [19] A. Bazzi, D. T. M. Slock, and L. Meilhac, "On spatio-frequential smoothing for joint angles and times of arrival estimation of multipaths," *ICASSP*, 2016.
- [20] D. Alibi, U. Javed, et al., "2D DOA estimation method based on channel state information for uniform circular array," in *Proc. Int. Conf. Ubiquitous Positioning Indoor Navigation and Location Based Services (UPINLBS)*, 2016, pp. 68–72.
- [21] F. Wen, Q. Wan, R. Fan, and H. W. Wei, "Improved MUSIC algorithm for multiple noncoherent subarrays," *IEEE Signal Process. Lett.*, vol. 21, no. 5, pp. 527–530, 2014.
- [22] W. Xie, C. Wang, F. Wen, J. Liu and Q. Wan, "DOA and gain-phase errors estimation for noncircular sources with central symmetric array," *IEEE Sensors Journal*, vol. 17, no. 10, pp. 3068–3078, May 2017.
- [23] W. Xie, F. Wen, J. Liu, and Q. Wan, "Source association, DOA and fading coefficients estimation for multipath signals," *IEEE Trans. Signal Process.*, vol. 65, no. 11, pp. 2773–2786, June 2017.
- [24] F. Wen, P. Liu, H. Wei, Y. Zhang, and R. C. Qiu, "Joint azimuth, elevation, and delay estimation for 3D indoor localization," *IEEE Trans. Vehicular Technology*, to be published, 2018.
- [25] P. Stoica and A. Nehorai, "Music, maximum likelihood, and Cramer–Rao bound," *IEEE Trans. Acoust., Speech, Signal Process.*, vol. 37, pp. 720–743, May 1989.
- [26] F. Wen and Q. Wan, "Maximum likelihood and signal-selective TDOA estimation for noncircular signals," *Journal of Communications and Networks*, vol. 15, no. 3, pp. 245–251, June 2013.
- [27] F. Wen, Q. Wan, and L. Y. Luo, "Time-difference-of-arrival estimation for noncircular signals using information theory," *Int. Journal Electronics Communications*, vol. 67, no. 3, pp. 242–245, 2013.
- [28] F. Wen, Q. Wan "Robust time delay estimation for speech signals using information theory: A comparison study," *EURASIP Journal on Audio, Speech, and Music Processing*, vol. 2011, no. 1, pp. 1–10, 2011.
- [29] I. Ziskind and M. Wax, "Maximum likelihood localization of multiple sources by alternating projections," *IEEE Trans. Acoust., Speech, Signal Process.*, vol. 36, pp. 1553–1560, Oct. 1988.